Impact of gas-solid direct contact on gas-liquid-solid reaction performance in a flow reactor

Asano, Shusaku
Institute for Materials Chemistry and Engineering, Kyushu University

Miyamura, Hiroyuki
Interdisciplinary Research Center for Catalytic Chemistry, National Institute of Advanced Industrial Science and Technology (AIST)

Matsushita, Mizuki
Interdisciplinary Graduate School of Engineering Sciences, Kyushu University

Kudo, Shinji
Institute for Materials Chemistry and Engineering, Kyushu University

他

出版情報：Journal of the Flow Chemistry. 14, pp.329-335, 2023-11-28. Springer Nature
バージョン：

Impact of gas-solid direct contact on gas-liquid-solid reaction performance in a flow reactor

Shusaku Asano[1,2*], Hiroyuki Miyamura[3*], Mizuki Matsushita[2], Shinji Kudo[1],

Shū Kobayashi[4*], Jun-ichiro Hayashi[1,2]

1. Institute for Materials Chemistry and Engineering, Kyushu University, Kasuga, Fukuoka 816-8580, Japan
2. Interdisciplinary Graduate School of Engineering Sciences, Kyushu University, Kasuga, Fukuoka 816-8580 Japan
3. Interdisciplinary Research Center for Catalytic Chemistry, National Institute of Advanced Industrial Science and Technology (AIST), Tsukuba, Ibaraki 305-8565, Japan
4. Department of Chemistry, School of Science, The University of Tokyo, Hongo, Bunkyo-ku, Tokyo 113-0033, Japan

*E-mail: asano.syusaku.392@m.kyushu-u.ac.jp, h.miyamura@aist.go.jp, shu_kobayashi@chem.s.u-tokyo.ac.jp

Abstract

Although gas-liquid-solid reactions, such as catalytic hydrogenation, have a long history, a fundamental understanding of the flow behavior and its effect on the reaction is lacking for flow chemistry applications using powder catalysts. This study revealed the distinctive effect of gas-solid direct contact on the surface of a powder catalyst. Direct gas–solid contact accelerates the reaction beyond the theoretical maximum of the batch reaction system, where gaseous species are supplied to the catalyst surface after dissolution into the liquid. The benefit of direct contact is further pronounced in systems with low-solubility gaseous species. Liquid holdup analysis revealed that the microconcavities of the catalyst support is crucial for sustaining the liquid using capillary forces and supplying the liquid substrate to the catalyst surface even under high G/L conditions. The gas-to-liquid flow rate ratio (G/L) is a decisive factor for direct gas–solid contact, whereas the flow direction, whether upflow or downflow, has no impact on powder catalysts with a size of a few hundred microns.

Keywords

Flow reactor: Hydrogenation: Powder catalyst: Mass transfer: Liquid holdup

Highlights

・Utilization of a powder catalyst in flow reactor enables direct gas-solid contact.

・Accelerated reactions through gas-solid direct contact surpass the maximum rate in the reaction-controlled regime.

・Micro-concavities of particles plays crucial role for retaining liquid in a reactor and achieve stable reaction rate.

1 Introduction

In recent years, flow chemistry utilizing solid catalysts has garnered significant attention in the field of organic synthesis owing to its advantages in productivity, low separation costs, and reduced environmental impacts [1]. Although the practice of employing columns packed with solid catalysts dates back a century in the domain of petroleum chemistry, the context of flow chemistry demands a departure from conventional conditions. For example, in petroleum chemistry, catalysts typically take the form of molded or pelletized structures, requiring dimensions of several millimeters to accommodate throughputs exceeding tens of tons per day. The use of a powder catalyst is inhibited owing to the large pressure drop [2]. Conversely, the landscape of flow chemistry in organic synthesis permits the effective use of fine powder catalysts down to the micron scale [3] owing to the feasible production range of grams to kilograms per day.

The majority of fundamental studies on gas-liquid-solid reactions have been conducted using molded catalysts with dimensions in the millimeter range [4–6]. Although there have been pioneering efforts involving micro-packed bed reactors [7,8], the systematic design of packed bed reactors for flow chemistry remains challenging. For instance, the flow direction of the gas and liquid streams to the reactor (upflow or downflow) is one of the most important design factors for a conventional packed bed reactor, and many studies have reported the advantages and disadvantages of using each direction [5,9–11]. In brief, the upflow condition results in better thermal stability owing to the higher liquid holdup than the downflow [9] and a higher reaction rate owing to the better mixing quality with upward bubble movement [5]. However, the downflow condition can reduce the pressure drop due to gravity [10]. Although it is believed that flow direction is important for flow chemistry applications [2], it is decided empirically by each research group and manufacturing company [12,13].

The contributions of Miyamura et al. have unveiled previously uncharted aspects of gas-liquid-solid reactions in packed bed reactors [14]. They performed hydrogenation reactions of arenes with fine powder catalysts and demonstrated that reaction rates in flow reactors surpassed those attainable in batch reactors by factors ranging from five-fold up to an astonishing twenty-seven-fold. Remarkably, the observed acceleration in their study did not originate from the typical mechanisms of enhanced mass transfer at the gas-liquid interface, which is a conventional advantage of flow reactors over batch reactors [15]. In fact, the reaction

rate in the flow reactors exceeded the theoretical maximum rate achievable in the reaction-controlling regime, as verified through the model calculations in this study. Detailed descriptions of this topic are provided in the Supporting Information along with the model equations. While Miyamura et al. postulated that direct gas-solid contact within the packed bed reactor contributes to the enhanced reaction rate, this hypothesis still awaits empirical validation.

This study was motivated by the aspiration to unravel the intricate mechanisms governing the acceleration of gas-solid-liquid reactions within powder catalyst-packed reactors, where direct gas-solid contact emerges as a pivotal factor. Our investigation delves into the flow behavior and reaction performance to shed light on the origins of gas-solid contact and its impact on the reaction.

2 Methodology

2.1 Materials

A polysilane-immobilized Rh–Pt bimetallic catalyst was prepared following the procedure outlined in a previous study [14]. Briefly, the metal precursors were reduced using $NaBH_4$ in a suspension of polydimethylsilane (DMPSi) in tetrahydrofuran. After 1 h of mixing, Al_2O_3 particles (basic alumina 90, Merck) were added to the suspension and kept for 2 h. Following methanol addition, filtration, drying, and rigorous washing resulted in bimetallic Rh–Pt nanoparticles supported on DMPSi, which were further supported by Al_2O_3. The Rh and Pt loadings were measured using inductively coupled plasma atomic emission spectroscopy (ICP-AES) following digestion with aqua regia. The Rh and Pt loadings were 0.072 and 0.060 mmol/g, respectively. The Rh-Pt/(DMPSi-Al_2O_3) catalyst used in the previous study had a different metal composition and higher catalytic activity than those used in the current investigation. The pore size distribution of the Al_2O_3 particles was measured using a mercury intrusion porosimeter (Autopore V9620, Micrometrics). The results are shown in the Supporting Information. The particle size of Al_2O_3, as provided by Merck, is reported to range between 63–200 μm.

2.2 Hydrogenation of toluene

For the flow hydrogenation experiments, 200 mg of the Rh-Pt/(DMPSi-Al_2O_3) catalyst was combined with 1800 mg of Al_2O_3 to yield a diluted catalyst mixture. A portion of the diluted

catalyst (977 mg) was packed into a glass column with a diameter of 5 mm and a length of 53 mm. A filter paper was placed on both ends of the column to retain the catalyst. A tube-in-tube structure was used for the liquid and gas inlets. Neat toluene was fed from the inner tube, and H_2 gas was fed from the outer tube. The outlet tubing was placed in an ice bath to prevent any loss of products or residual reactants owing to vaporization. The effluent solution from the reactor was collected from the outlet and subsequently subjected to gas chromatography. Only methylcyclohexane and toluene peaks were observed in the chromatograms. The toluene conversion was determined using the area ratio of these two peaks and the response factors of toluene and methylcyclohexane. Given that the hydrogenation of toluene adheres to a zero-order rate law concerning the toluene concentration [14,16], the turn-over frequency (TOF) in the flow reactor was deduced by dividing the methylcyclohexane output by the molar amount of Rh in the reactor. Gas phase hydrogenation was conducted with another flow type reactor. Details of the gas phase hydrogenation setup is described in the Supporting Information. The method used for the batch experiments is also described in the Supporting Information.

2.3 Liquid holdup analysis

The liquid holdup within the column was assessed by analyzing the impulse response after the introduction of a tracer. The experimental setup is illustrated in Figure 1. In this setup, neat toluene, which served as a tracer and was detectable via UV absorption at 254 nm, was injected into the liquid stream of ethyl acetate. Al_2O_3 (Merck, 1.068 g) were used as substitutes for Rh-Pt/(DMPSi-Al_2O_3) to prevent tracer adsorption onto the column contents. To minimize the influence of the external residence time on the column, a surplus quantity of heptane was introduced at the column outlet. A gas-liquid separator (SEP-10, Zaiput) was placed before the UV detector to prevent the introduction of hydrogen gas into the detector. Bypass measurements were conducted in the absence of a column. Experiment with a glass bead packing was conducted for a comparison.

The mean residence time of the liquid was determined from the UV absorption profile and subsequently refined by subtracting the mean residence time of the bypass measurement from that of the measurement involving the column. The liquid volume within the column was calculated as the product of the mean residence time and liquid flow rate. The liquid holdup was calculated as the volume fraction of liquid within the column divided by the bed porosity. The density of Al_2O_3, documented at 3.94 g/mL, was used for bed porosity calculation with the empty column volume and the packed amount of Al_2O_3. Notably, these measurements were

executed in an automated fashion, facilitated by proprietary software developed in our previous work [17–19].

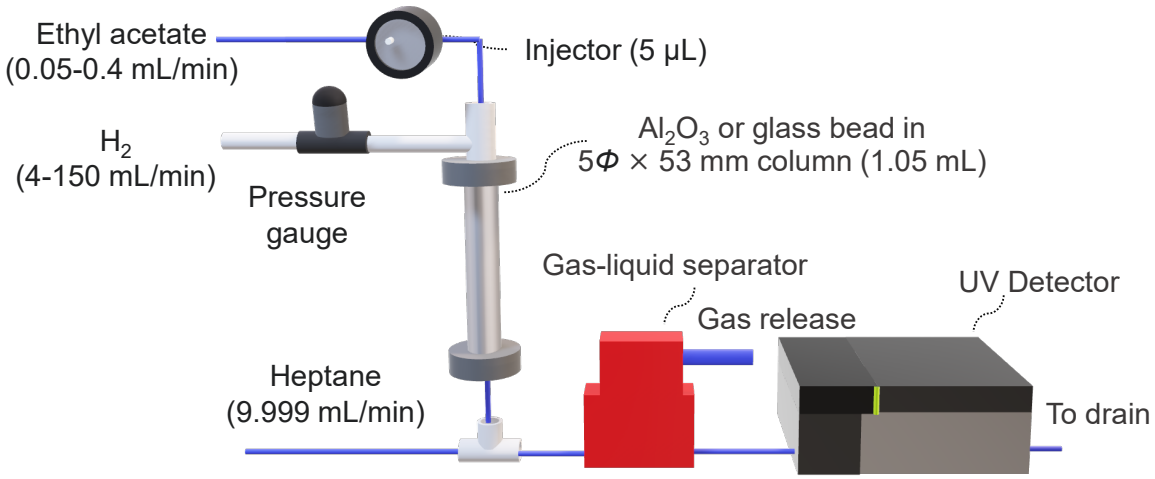

Figure 1. Setup for measuring the residence time distribution

3 Results

Figure 2(a) shows the hydrogenation rates under various operating conditions. The *x*-axis is the ratio of the gas flow rate under standard conditions to the liquid flow rate (G/L). By examining the range of G/L values below 100, it becomes apparent that G/L is the dominant factor. Increasing the G/L ratio led to a notable increase in TOF from 300 to approximately 500. TOF in batch reactor is as small as 124 and the exceling performance of the flow reactor was confirmed. As G/L surpassed 100, the TOF values ranged from 430 to 580 without a clear correlation with the operational conditions. Gas phase reaction resulted the TOF value of 522. The flow direction, whether upflow or downflow, had no significant effect on the TOF.

Figure 2(b) shows the pressure drop. An increase in both the liquid and gas flow rates corresponds to an increase in the pressure drop. The pressure-drop profile did not mirror the TOF profile, thus confirming that the pressure within the column was not responsible for the reaction rate acceleration observed in the flow reactor. Notably, in contrast to the note in a 2009 review of conventional packed bed reactors asserting that "particle size cannot be smaller than 1 mm due to pressure drop" [20], the pressure drop in our operation range is quite small owing to the small liquid superficial velocity, the short column length, and the least swelling property of the solid catalysts.

The flow direction had no discernible influence on the pressure drop. While the influence of the flow direction is pronounced in systems featuring structured catalysts larger than several

millimeters, this effect is predominantly governed by gravity. Conversely, for packing dimensions below several hundred microns, the gravitational force loses significance compared to the inertial, viscous, and capillary forces [7]. Hence, the flow direction did not affect either the reaction outcome or the pressure drop within the packed bed reactor employing the powdered catalyst.

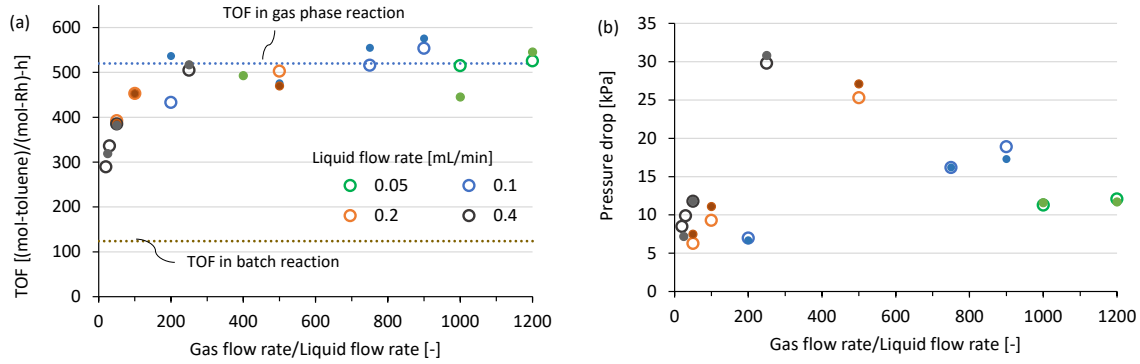

Figure 2. Toluene hydrogenation performance at 50°C as a function of gas/liquid volume flow rate ratio: (a) TOF, and (b) pressure drop. Open circles represent upflow conditions, while filled circles denote downflow conditions.

The reaction rate in the flow reactor was intensified with the increase of G/L to the level of gas phase reaction. From Figure 2(a), it is reasonable to assume that the catalyst is dried with the increase of G/L and gaseous hydrogen directly contact to catalyst surface. However, previous studies for gas-liquid-solid reaction reported that drying of the catalyst surface by a high gas flow rate reduces reaction rate [21–23]. This is because liquid substrate is rapidly ejected from the reactor by a gas stream and contact of the catalyst and substrate becomes insufficient. If the enhanced TOF in our case is due to the gas-solid contact, there should be another key phenomenon that maintain the sufficient contact of the catalyst and substrate. Thus, we examined the liquid holdup in the Al_2O_3 packed column to investigate whether the gas-solid direct contact can exist without liquid expulsion. Figure 3 summarizes the liquid holdup in the packed bed reactor as determined by residence time analysis. The liquid holdup profile is analogous to the TOF profile in Figure 2(a). As the G/L ratio increased, the liquid holdup decreased in the range of G/L values below 100. For G/L values greater than 100, the liquid holdup remains consistent, ranging from 0.58 to 0.65 without a clear correlation with G/L.

The glass bead packing resulted in a totally different liquid holdup profile as shown in the Supporting Information. A monotonic reduction in the liquid holdup with an increase in the

gas flow rate was observed with in the case of glass bead. A small liquid flow rate of 0.05 mL/min resulted in a minimum liquid holdup of 0.24. The high liquid holdup values in Figure 3 retained even with the large G/L is attributed to the distinctive nature of the Al_2O_3 particles. As described in the Supporting Information, the Al_2O_3 particles exhibit surface roughness with micro-concavities ranging from 10 to 50 μm and a volume of 0.49 mL/g. By packing 1.068 g of Al_2O_3 into the column, the cumulative volume of microconcavities within the column was 0.52 mL. If the entire volume of these microconcavities was assumed to be filled with liquid, the corresponding liquid holdup value was calculated as 0.68. Hence, the high liquid holdup values even under conditions of high G/L values, can be attributed to the retention of liquid within these micro-concavities. Capillary force acts between the liquid phase and the Al_2O_3 surface, thus mitigating the expulsion of the liquid even under conditions of elevated G/L.

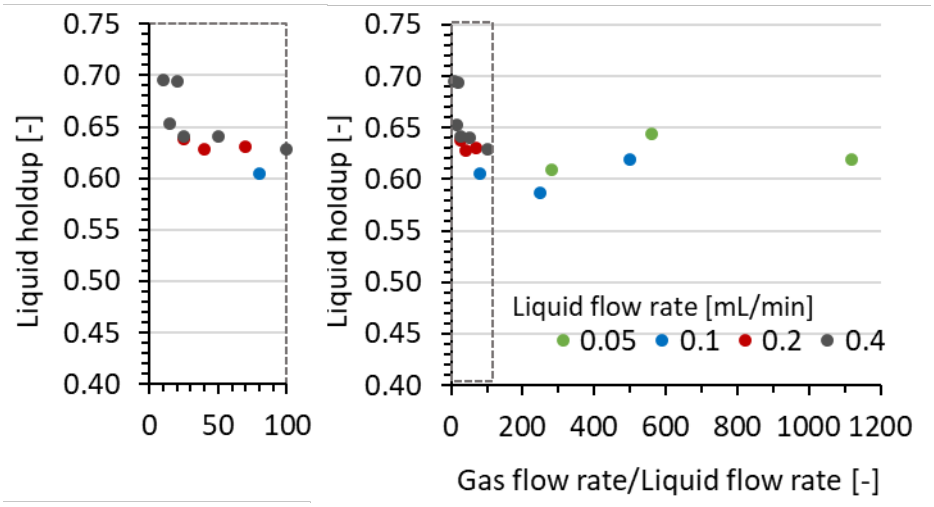

Figure 3. Liquid holdup in the column packed with Al_2O_3. Plots at small G/L is enlarged for better visibility.

4 Discussions

At the microscopic level, the hydrogenation reaction rate follows the principles of the Langmuir-Hinshelwood mechanism, which is a function of the surface concentrations of adsorbed toluene and hydrogen [24]. The adsorption constant of toluene significantly surpassed that of hydrogen [25]. Consequently, increasing the hydrogen concentration on the catalyst surface is crucial for increasing the reaction rate. Figure 4 illustrates the H_2 transfer mechanism based on the experiments conducted in this study. In a batch reactor, H_2 must be dissolved in liquid before it reaches the active sites of the catalyst, as shown in Figure 4(a). This requirement significantly limits the reaction performance because the H_2 solubility of

toluene at 50°C with 1 bar H_2 is as low as 4 mmol/L. Even after vigorous stirring to augment H_2 dissolution from the gas to the liquid, the catalyst surface was poor in hydrogen because it was in equilibrium with the hydrogen concentration in the liquid. Conversely, as shown in Figure 4(b), the flow reactor offered a direct supply of hydrogen from the gas phase. Given that the Rh-Pt catalyst is supported by DMPSi and situated on the surface of Al_2O_3, it becomes exposed to the gas phase when the G/L ratio is sufficiently high. Consequently, the hydrogen concentration at the active sites of the catalyst significantly surpasses that in the liquid phase. Supply route of liquid substrate can be through infiltration into the DMPSi matrix or evaporation to the gas phase. Considering that hydrogenation of N-methylaniline, which has much higher boiling point of 196°C than toluene (110.6°C), resulted in much higher TOF in the flow system (Table 1), supply of the substrate to the catalyst as the liquid would be the dominant path.

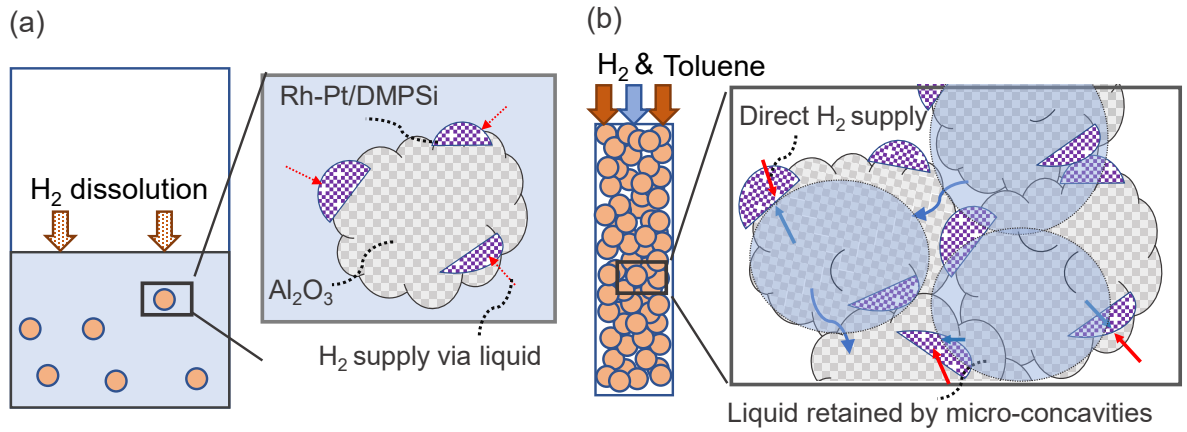

Figure 4. Schematic comparison of hydrogen supply route to the catalyst active site: (a) batch reactor, and (b) flow reactor with high gas/liquid ratio (G/L).

According to the principle that direct contact of a gas with the catalyst surface increases the surface hydrogen concentration and, consequently, the reaction rate, the extent of reaction rate acceleration should be notably pronounced in systems with diminished H_2 solubility. This phenomenon is corroborated by Table 1, which compares the H_2 solubilities of the four arene substrates with their reported TOF values. Substrates exhibiting poorer H_2 solubility, particularly N-containing substrates, manifested the most substantial reaction acceleration in the flow reactor compared to the batch reactor. It is worth emphasizing that the impact of direct contact of the gas with the catalyst surface is completely different from the usual reaction acceleration caused by enhanced mass transfer at the gas-liquid interface [15,26]. In the latter scenario, it is difficult to improve the slower reaction because the slower reaction at the catalyst

surface is less affected by the mass transfer rate at the gas-liquid interface. As shown in Table 1, the slower reactions of N-methylaniline and pyrrole accelerated significantly compared to the faster reactions of toluene. The profound impact of the gas-solid direct contact effect in a powder catalyst-packed reactor holds pivotal significance in the development of efficient flow chemistry systems.

Table 1. Comparison of the H_2 solubility at 50°C and enhancement of TOF in a flow reactor.

Substrate	H_2 solubility[a] [mmol/L]	TOF [mol/(mol-Rh)-h][b]		
		in batch	in flow[c]	TOF-flow/TOF-batch
N-methylaniline	0.55	14	378	27
Pyrrole	0.58	22	593	27
o-Xylene	3.84	30	213	7.1
Toluene	4.58	221	1189	5.4

[a] Estimated by a process simulator (ASPEN HYSYS) with the UNIQUAC model.

[b] Values in the previous study [14].

[c] G/L range is 1100–1300.

5 Conclusions

In this study, we investigated the underlying factors driving the accelerated hydrogenation observed in a flow reactor employing powder catalysts. The following conclusions were drawn:

(1) The deployment of a flow reactor packed with powder catalysts facilitates direct gas-solid contact, leading to a remarkable acceleration of reaction rates. The reaction rate in flow reactor surpasses the limits imposed by the conventional gas supply route involving gas-liquid and liquid-solid interfaces and reaches to the level of the gas phase reaction. This enhancement was particularly pronounced in reaction systems characterized by poor hydrogen solubility in the liquid phase.

(2) G/L dominates gas-solid direct contact and subsequent reaction acceleration within the examined conditions—liquid flow rates ranging from 0.05 to 0.4 mL/min and gas flow rates spanning 8 to 100 mL/min for a reactor diameter of 5 mm. The flow direction had no impact on the reaction outcomes when powder catalysts with dimensions below several hundred microns were employed.

(3) The surface roughness of the supporting Al_2O_3 retained the liquid within the reactor even at elevated G/L ratios ranging from 100 to 1000. The ability of Al_2O_3 to hold liquids helps ensure a consistent supply of the liquid substrate to the active sites of the catalyst.

To advance flow chemistry technologies, further investigations should delve into the design and operational strategies that maximize the gas-solid direct contact effect across various reaction systems and reactor scales.

Conflict of interest

There is no conflict of interest to declare.

Acknowledgement

This work was supported by JSPS KAKENHI (grant numbers JP21H05083 and JP21H05082) and Joint Usage/Research Center for Catalysis. (Proposal #23CY0303). SA and SK acknowledge the support of the Cooperative Research Program of the Network Joint Research Center for Materials and Devices, supported by the Ministry of Education, Culture, Sports, Science, and Technology (MEXT), Japan. SA and HM acknowledge support from the Research and Education Grant for the University Consortium (Consortium name: CES-CHEM).

Supporting information

The following supporting information is available: reaction rate acceleration analysis using a conventional gas-liquid mass transfer enhancement model and porosity analysis of the Al_2O_3 support (PDF).

References

[1] M. B. Plutschack, B. Pieber, K. Gilmore, P. H. Seeberger, The Hitchhiker's Guide to Flow Chemistry, Chem. Rev. 117 (2017) 11796–11893. https://doi.org/10.1021/acs.chemrev.7b00183.

[2] E. Masson, E.M. Maciejewski, K.M.P. Wheelhouse, L.J. Edwards, Fixed Bed Continuous Hydrogenations in Trickle Flow Mode: A Pharmaceutical Industry Perspective, Org. Process Res. Dev. 26 (2022) 2190–2223. https://doi.org/10.1021/acs.oprd.2c00034.

[3] N. Cherkasov, P. Denissenko, S. Deshmukh, E.V. Rebrov, Gas-liquid hydrogenation in continuous flow – The effect of mass transfer and residence time in powder packed-bed

and catalyst-coated reactors, Chem. Eng. J. 379 (2020) 122292. https://doi.org/10.1016/j.cej.2019.122292.

[4] T. Murugesan, V. Sivakumar, Liquid Holdup and Interfacial Area in Cocurrent Gas-Liquid Upflow through Packed Beds, J. Chem. Eng. Jpn. 38 (2005) 229–242. https://doi.org/10.1252/jcej.38.229.

[5] A.J. Van Houwelingen, W. Nicol, Parallel hydrogenation for the quantification of wetting efficiency and liquid-solid mass transfer in a trickle-bed reactor, AIChE J. 57 (2011) 1310–1319. https://doi.org/10.1002/aic.12342.

[6] A.V. Raghavendra Rao, R. Kishore Kumar, T. Sankarshana, A. Khan, Identification of Flow Regimes in a Concurrent Gas Liquid Upflow through Packed Beds, Chem. Eng. Technol. 34 (2011) 1909–1917. https://doi.org/10.1002/ceat.201100070.

[7] J. Zhang, A.R. Teixeira, L.T. Kögl, L. Yang, K.F. Jensen, Hydrodynamics of gas-liquid flow in micropacked beds: Pressure drop, liquid holdup, and two-phase model, AIChE J. 63 (2017) 4694–4704. https://doi.org/10.1002/aic.15807.

[8] W. Liu, B. Xie, C. Zhang, X. Duan, J. Zhang, Nature and characteristics of gas–liquid flow regimes in a micro-packed bed reactor, AIChE J. 69 (2023) e18004. https://doi.org/10.1002/aic.18004.

[9] I. Iliuta, F. Larachi, Three-phase fixed-bed reactors, in: Z.I. Önsan, A.K. Avci (Eds.), Multiph. Catal. React., John Wiley & Sons, Inc., Hoboken, NJ, USA, 2016: pp. 95–131. https://doi.org/10.1002/9781119248491.ch5.

[10] Y. Wu, M.R. Khadilkar, M.H. Al-Dahhan, M.P. Dudukovic, Comparison of Upflow and Downflow Two-Phase Flow Packed-Bed Reactors with and without Fines: Experimental Observations, Ind. Eng. Chem. Res. 35 (1996) 397–405.

[11] J. Tan, Y.-N. Ji, W.-S. Deng, Y.-F. Su, Process intensification in gas/liquid/solid reaction in trickle bed reactors: A review, Pet. Sci. 18 (2021) 1203–1218. https://doi.org/10.1016/j.petsci.2021.07.007.

[12] R.V. Jones, L. Godorhazy, N. Varga, D. Szalay, L. Urge, F. Darvas, Continuous-Flow High Pressure Hydrogenation Reactor for Optimization and High-Throughput Synthesis, J. Comb. Chem. 8 (2006) 110–116. https://doi.org/10.1021/cc050107o.

[13] M. Itoda, Y. Naganawa, M. Ito, H. Nonaka, S. Sando, Structural exploration of rhodium catalysts and their kinetic studies for efficient parahydrogen-induced polarization by side arm hydrogenation, RSC Adv. 9 (2019) 18183–18190. https://doi.org/10.1039/C9RA02580D.

[14] H. Miyamura, A. Suzuki, T. Yasukawa, S. Kobayashi, Polysilane-Immobilized Rh-Pt Bimetallic Nanoparticles as Powerful Arene Hydrogenation Catalysts: Synthesis, Reactions under Batch and Flow Conditions and Reaction Mechanism, J. Am. Chem. Soc. 140 (2018) 11325–11334. https://doi.org/10.1021/jacs.8b06015.

[15] J. Tu, L. Sang, H. Cheng, N. Ai, J. Zhang, Continuous Hydrogenolysis of N-Diphenylmethyl Groups in a Micropacked-Bed Reactor, Org. Process Res. Dev. 24 (2020) 59–66. https://doi.org/10.1021/acs.oprd.9b00416.

[16] F. Alshehri, H.M. Weinert, S.D. Jackson, Hydrogenation of alkylaromatics over Rh/silica, React. Kinet. Mech. Catal. 122 (2017) 699–714. https://doi.org/10.1007/s11144-017-1251-6.

[17] K. Igawa, S. Asano, Y. Yoshida, Y. Kawasaki, K. Tomooka, Analysis of Stereochemical Stability of Dynamic Chiral Molecules Using an Automated Microflow Measurement System, J. Org. Chem. 86 (2021) 9651–9657. https://doi.org/10.1021/acs.joc.1c00914.

[18] S. Asano, Y. Takahashi, T. Maki, Y. Muranaka, N. Cherkasov, K. Mae, Contactless mass transfer for intra-droplet extraction, Sci. Rep. 10 (2020) 7685. https://doi.org/10.1038/s41598-020-64520-4.

[19] Y. Muranaka, T. Maki, D. Nakayoshi, S. Asano, K. Ikebata, A. Nagaki, Y. Ashikari, K. Mandai, K. Mae, Continuous enantiomeric separation using water-oil-water segmented flow system, Chem. Eng. J. 469 (2023) 143891. https://doi.org/10.1016/j.cej.2023.143891.

[20] F.S. Mederos, J. Ancheyta, J. Chen, Review on criteria to ensure ideal behaviors in trickle-bed reactors, Appl. Catal. Gen. 355 (2009) 1–19. https://doi.org/10.1016/j.apcata.2008.11.018.

[21] N. Al-Rifai, F. Galvanin, M. Morad, E. Cao, S. Cattaneo, M. Sankar, V. Dua, G. Hutchings, A. Gavriilidis, Hydrodynamic effects on three phase micro-packed bed reactor performance – Gold–palladium catalysed benzyl alcohol oxidation, Chem. Eng. Sci. 149 (2016) 129–142. https://doi.org/10.1016/j.ces.2016.03.018.

[22] S. Tadepalli, R. Halder, A. Lawal, Catalytic hydrogenation of o-nitroanisole in a microreactor: Reactor performance and kinetic studies, Chem. Eng. Sci. 62 (2007) 2663–2678. https://doi.org/10.1016/j.ces.2006.12.058.

[23] R. Langsch, J. Zalucky, S. Haase, R. Lange, Investigation of a packed bed in a mini channel with a low channel-to-particle diameter ratio: Flow regimes and mass transfer in gas–liquid operation, Chem. Eng. Process. Process Intensif. 75 (2014) 8–18. https://doi.org/10.1016/j.cep.2013.10.004.

[24] N. Cherkasov, S. Asano, Y. Tsuji, K. Okazawa, K. Yoshizawa, H. Miyamura, J. Hayashi, A.A. Kunitsa, S.D. Jackson, Mechanistic origins of accelerated hydrogenation of mixed alkylaromatics by synchronised adsorption over Rh/SiO_2, React. Chem. Eng. 8 (2023) 1341–1348. https://doi.org/10.1039/D3RE00032J.

[25] T. Takahashi, K. Yamashita, T. Kai, I. Fujiyoshi, Hydrogenation of benzene, mono-, di-, and trimethylbenzenes over nickel catalysts supported on porous glass, Can. J. Chem. Eng. 64 (1986) 1008–1013. https://doi.org/10.1002/cjce.5450640619.

[26] J. Keybl, A microreactor system for high-pressure, multiphase homogeneous and heterogeneous catalyst measurements under continuous flow, 2011. http://dspace.mit.edu/handle/1721.1/70399.

Supporting Information

Impact of gas-solid direct contact on gas-liquid-solid reaction performance in a flow reactor

Shusaku Asano, Hiroyuki Miyamura, Mizuki Matsushita, Shinji Kudo,

Shū Kobayashi, Jun-ichiro Hayashi

Reaction rate acceleration beyond the reaction controlling regime

The conventional understanding of flow reactors highlights that enhancing the mass transfer at the gas-liquid interface yields higher reaction rates than in batch reactors, effectively transforming from the mass transfer controlling regime to the reaction-controlling regime. The kinetic analysis of arene hydrogenation shown in Figure S1 in a batch reactor with Rh–Pt/(DMPSi-Al_2O_3) powder catalysts indicate the importance of the mass transfer on this reaction. However, the acceleration in flow reactors utilizing the same Rh–Pt/(DMPSi-Al_2O_3) powder catalysts cannot be explained by a simple shift toward the reaction control regime.

The blue markers in Figure S1 indicate the experimental reaction rate against catalyst loading in a batch reactor with the Rh–Pt/(DMPSi-Al_2O_3) powder catalysts. The reaction rate was not proportional to the catalyst loading because of the influence of the mass transfer of H_2 at the gas-liquid interface in the reactor. The following model equations describe this effect: The hydrogenation of toluene in the liquid phase is known to be of the 0th order of toluene concentration and the 1st order of hydrogen concentration [16]. Thus, the rate of toluene consumption is:

$$r_{\mathrm{tol}} = k_{\mathrm{tol}} C_{\mathrm{H_2}} W \qquad \text{(Eq. 1)}$$

where k_{tol} is the rate constant, $C_{\mathrm{H_2}}$ is the hydrogen concentration in the liquid phase, and W is the catalyst loading. The rate of hydrogen consumption $r_{\mathrm{H_2}}$ equals to $3r_{\mathrm{tol}}$, according to the reaction equation of $C_7H_8 + 3H_2 \rightarrow C_7H_{14}$. The hydrogen supply rate from the gas phase to the liquid phase is

$$N_{\mathrm{H_2}} = k_{\mathrm{L}} A (C^*_{\mathrm{H_2}} - C_{\mathrm{H_2}}) \qquad \text{(Eq. 2)}$$

where k_{L} is the mass transfer coefficient, A is the specific surface area, and $C^*_{\mathrm{H_2}}$ is the saturated hydrogen concentration at a given temperature and H_2 pressure. Under the quasi-steady-state assumption, $N_{\mathrm{H_2}} = r_{\mathrm{H_2}}$ leading to

$$r_{\mathrm{tol}} = k_{\mathrm{tol}} W \frac{k_L A}{3k_{\mathrm{tol}} W + k_L A} C^*_{\mathrm{H_2}} \qquad \text{(Eq. 3)}.$$

When $k_L A \gg 3k_{\mathrm{tol}} W$, the reaction is in the chemical reaction controlling regime and Eq.3 approaches

$$r_{\mathrm{tol}} = k_{\mathrm{tol}} W C^*_{\mathrm{H_2}} \quad \text{(Eq. 4)}.$$

When $3k_{\mathrm{tol}} W \gg k_L A$, the reaction is in the mass transfer control regime, and Eq. 3 approaches

$$r_{\mathrm{tol}} = \frac{k_L A}{3} C^*_{\mathrm{H_2}} \text{ (Eq. 5)}.$$

The dashed curve in Figure S1 illustrates the model-fitting results obtained using Eq. 3, which are consistent with the experimental data, affirming the validity of the model. The blue lines in the figure represent Eq. 4 for the ideal case without mass-transfer limitations. The red line is for Eq. 5 in the mass transfer control regime. The constant value of the red line indicates the maximum mass transfer rate in the batch reactor, which sets the rate ceiling.

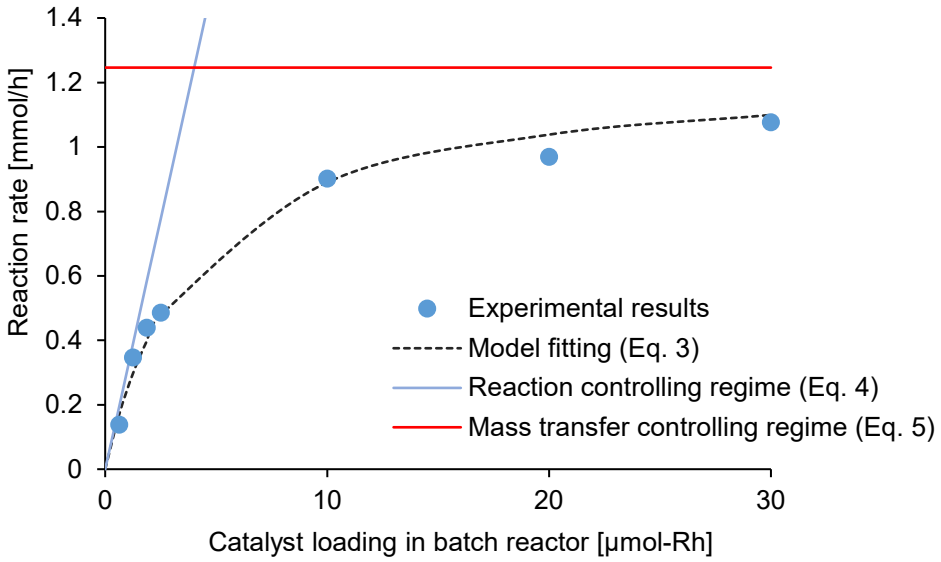

Figure S1. Effect of mass transfer in batch reactor reported in the previous study [14]. 10 mmol of toluene was hydrogenated at 50°C in a batch reactor with various catalyst loading.

If the reaction proceeded in the reaction control regime, the reaction rate was proportional to the catalyst loading, as shown by the blue line in Figure S1, whose slope indicates the inherent catalytic activity (TOF). Table S1 compares the TOF values from the model fitting to those from the flow and single-batch experiments. In an ideal reaction control scenario, the TOF registers a 40% increase compared to the smallest catalyst loading in a single-batch experiment. Remarkably, the TOF computed from flow experimentation is 3.8 times superior to the reaction control regime of a batch reactor. This indicates that the acceleration of reactions in a flow reactor stems from a cause beyond the augmentation of gas-liquid mass transfer.

Table S1. TOF values obtained from the experimental results in the previous study.

Batch experiment with 0.625 μmol-Rh loading	Slope value of blue line in Figure S1	Flow experiment with G/L of 1260
221	312	1189

Liquid holdup in a glass-bead-packed column

Glass bead with a diameter of 105-125 μm (BZ-01, AS ONE) was packed into a glass column with a diameter of 5 mm and a length of 53 mm. The packed amount was 1.607 g. Figure S2 summarizes the liquid holdup values for various liquid and gas flow rates.

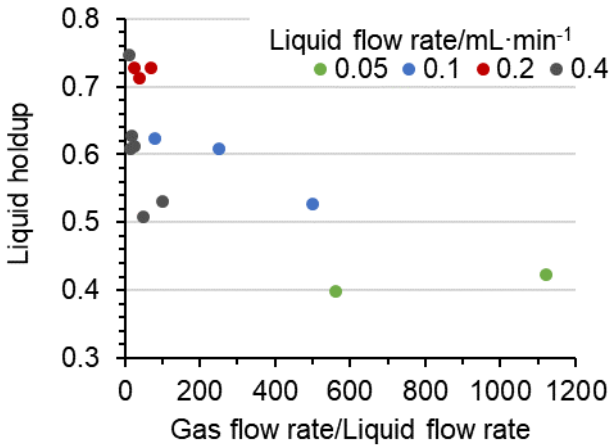

Figure S2. Liquid holdup in the column packed with glass bead.

Porosity analysis of Al_2O_3 support

Al_2O_3 particles (basic alumina 90, Merck) were used as the catalyst support and packing for residence time analysis. The particle size of Al_2O_3 is reported to be in the range of 63–200

μm by Merck. Figure S3 shows a microscopic image of Al_2O_3 captured using a digital microscope (VHX-900F, Keyence). They appear as non-spherical aggregate-like structures.

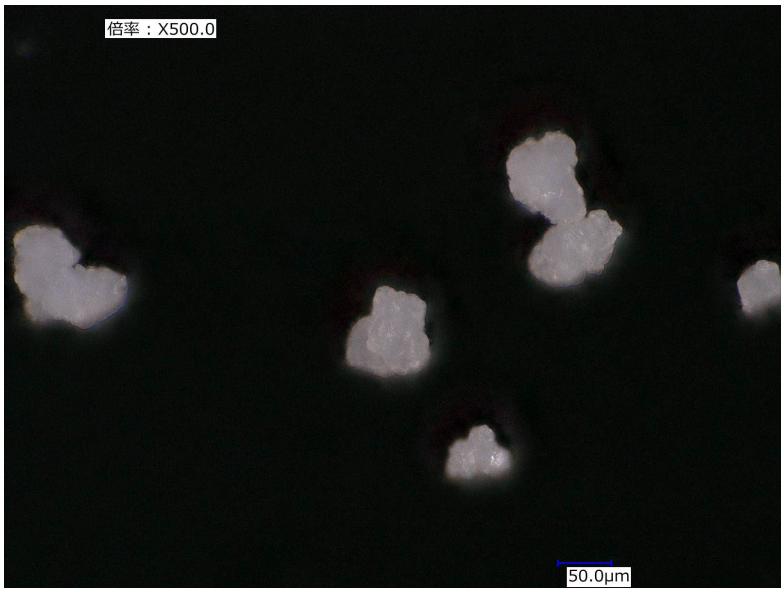

Figure S3. Microscopic image of Al_2O_3 used in this study.

The pore size distribution of the Al_2O_3 particles was measured using a mercury intrusion porosimeter (Autopore V9620, Micrometrics). Al_2O_3 particles weighing 0.3068 g were placed in the porosimeter after a 4-h drying period at 120°C. The results are shown in Figure S4. There are two distinct peaks at 3–10 nm and 10–50 μm. The former is a typical mesopore of ceramic materials, but the latter is not a typical pore, as no such large pores can be observed in Figure S3. Mercury intrusion porosimetry uses non-wetting liquid penetration to measure the size and volume of pores in a wide range of porous solids, and the microconcavities of the particle surface of Al_2O_3 can be detected as pores that reject mercury wetting. Therefore, it can be deduced that the Al_2O_3 particle bed exhibits surface roughness within the 10–50 μm range, with a corresponding volume of 0.49 mL/g.

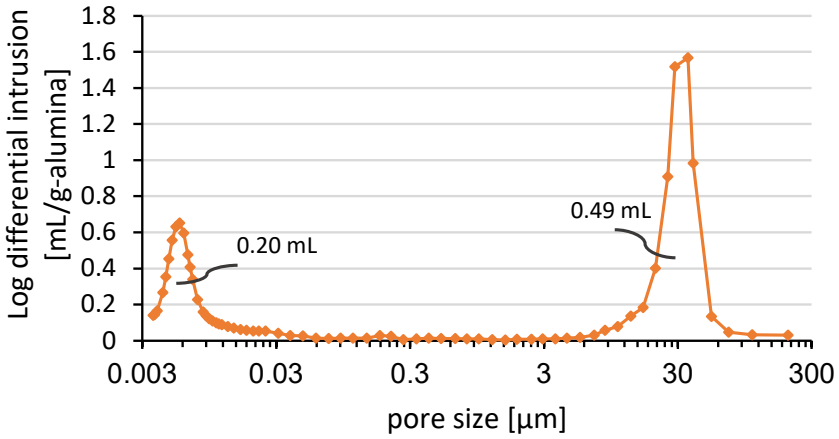

Figure S4. Pore size distribution of Al_2O_3 used in this study.

Hydrogenation in batch reactor

For the batch hydrogenation experiment, 36.5 mg of the Rh-Pt/(DMPSi-Al_2O_3) catalyst was placed in a two-necked test tube. A Schlenk line with H_2 flow (10 mL/min) was connected to one neck of the tube using a three-way cock, and the other neck was hermetically sealed with a cock equipped with a septum for sampling purposes. The ambient atmosphere was purged with H_2 to create an atmospheric H_2 environment. Subsequently, toluene (0.494 g) was injected into the test tube. The test tube was then introduced into the Carousel® system, which regulated the reaction temperature at 50°C by heating the tube's bottom while simultaneously cooling the middle portion to 5°C to prevent toluene evaporation. The reaction mixture was then stirred at 200 rpm. Sample aliquots were acquired using a gas-tight syringe, filtered, and subjected to gas chromatography (GC) using a GC-2030 instrument (Shimadzu) equipped with a TC-1701 column (GL Science) and a flame ionization detector. Figure S5 shows the conversion profile of the batch reactor. The TOF in the batch reactor was obtained by dividing the slope of the toluene conversion curve by molar ratio of toluene and Rh, as the reaction follows the 0^{th}-order rate law.

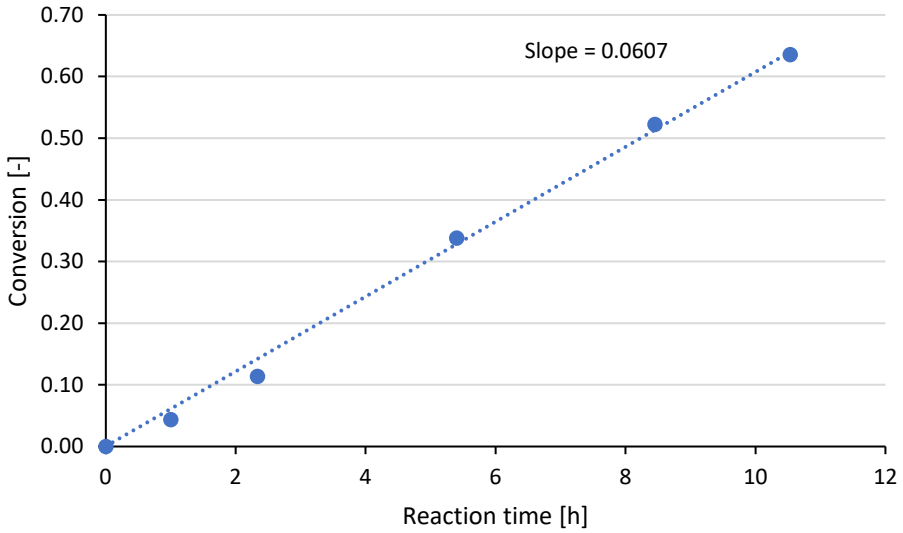

Figure S5. Reaction profile of toluene hydrogenation in batch reactor.

Hydrogenation in gas phase

Gas phase hydrogenation was conducted in a flow reactor system with an evaporation part as shown in Figure S6. Excess amount of hydrogen gas was mixed with a liquid flow of toluene to achieve complete evaporation at the reaction temperature. The evaporation coil was made of stainless steel with an outer diameter of 1/16". The outlet tubing was placed in an ice bath to condense toluene and methylcyclohexane.

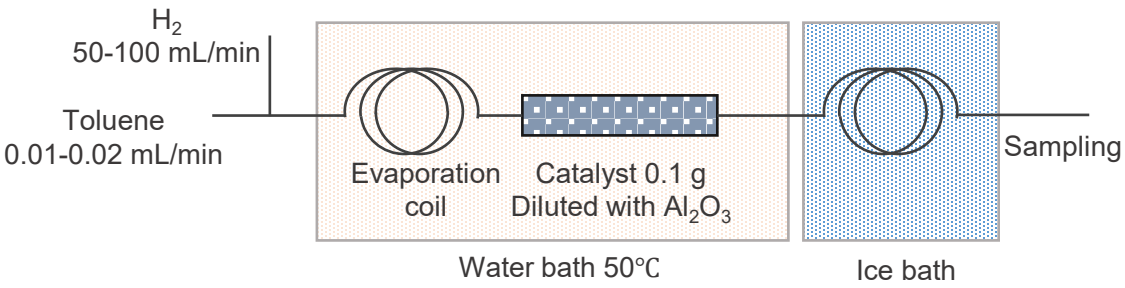

Figure S6. Reactor setup for gas phase hydrogenation.

Figure S7 shows the conversion profile in the gas phase against the moles hourly space velocity (MHSV). Calculation of MHSV is based on the Rh amount in the reactor so that the slope gives the TOF.

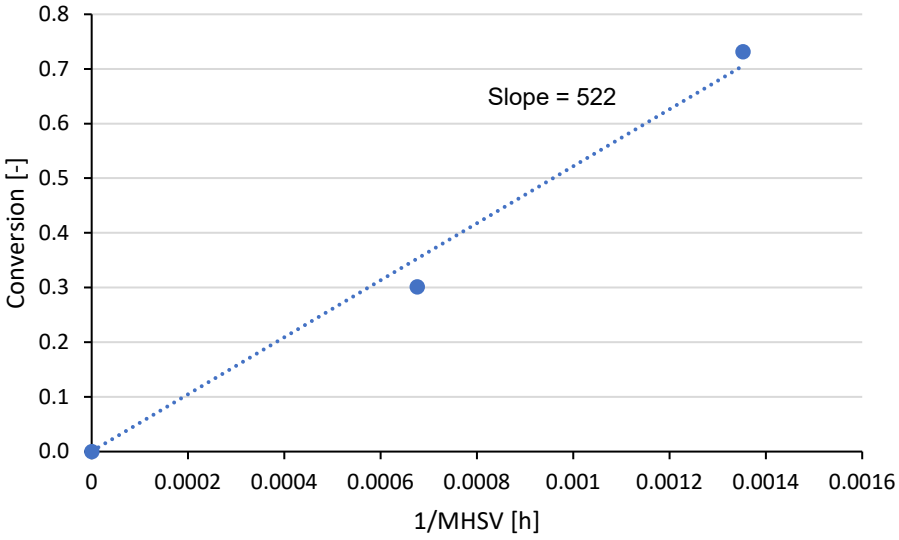

Figure S7. Reaction profile of toluene hydrogenation in the gas phase.